Vibration mitigation using an inerter-based isolation system

S.S. Abolghasemi & N.E. Wierschem
The University of Tennessee, Knoxville, Tennessee, U.S

J.B. Knight
NASA Marshall Space Flight Center, Huntsville, Alabama, U.S

ABSTRACT: Extreme dynamic environments can result in the failure of structures and equipment. To mitigate these effects, isolation systems can be used. In recent years, inerters have been studied as a part of different structural control methods. The inerter is attractive for many structural control methods because it can produce large mass effects despite having a small physical mass through the transformation of translational motion to the rotational motion of a flywheel. While inerters have been considered in structural control, experimental studies of isolation systems featuring inerters has been limited. This project seeks to study the ability of the addition of an inerter to improve the dynamic performance of isolation systems when considering a random vibration environment. The results of this study demonstrate that the inerter can have a large impact on the dynamic properties of an isolated system, including shifting the isolation mode frequency lower while reducing its amplitude. High frequency noise did result from the inclusion of the inerter but may not be of significant concern depending on the frequency range of interest. The strong performance of the inerter in a simplified isolation system observed during this work motivates future studies of inerters in isolation systems.

1 INTRODUCTION

High vibration environments can result in damage to or loss of functionality of structures and equipment. Structural control techniques, including isolation, can be utilized to lessen the effects of these environments. Inerters have been researched as part of many structural control techniques as they can produce considerable mass effects despite potentially having little physical mass. Inerters produce these mass effects by converting linear motion to the rotational motion of a flywheel.

The inerter was introduced by Smith (Smith 2002) as an element that could generate a force proportional to the relative acceleration between its nodes. The initial physical use of the inerter was in Formula 1 racing car suspension systems, where it was referred to as the J damper (Chen et al. 2009). Investigations have been done to show the influence of inerters on the natural frequencies of a single-degree-of-freedom (SDOF) and multi-degree-of-freedom (MDOF) vibration systems and verified the efficiency of inerters in reducing the dominant natural frequency (Chen et al. 2014).

Inerter-based structural control devices have been studied in which an inerter is used in conjunction with a significant supplemental physical mass. Typically, these systems can be described as inerter-based tuned mass dampers. Examples of these include the rotational inertial double tuned mass damper (Javidialesaadi & Wierschem, 2018), which features an inerter between the TMD mass and the main structure, and the tuned mass damper inerter (Marian & Giaralis, 2014), which features an inerter between the TMD mass and the ground.

Additionally, inerter-based structural control devices that are not used in conjunction with a large supplemental mass have been studied. An example of this is the tuned viscous mass damper, which was studied by Ikago et al. (Ikago et al. 2012). The inerter in this device was implemented experimentally using a ball-screw mechanism. This work serves to demonstrate the large mass amplification that is possible with an inerter as the device produces an effective mass of 350kg by using a flywheel that weighed only 2kg.

Using inerters in base isolation systems as a solution for vibration mitigation in buildings has been recently proposed (Wang et al. 2007 & 2009). A comparison of the isolated and non-isolated structure's frequency response curves has revealed a significant drop in the transmissibility coefficient throughout a wide frequency range (Salvatore et al. 2020).

Although numerical investigations have been done to examine the effectiveness of the inerter-based isolation in buildings, experimental studies and studies considering the effectiveness of inerters for equipment isolation are lacking.

This paper features the experimental investigation of an inerter-base isolation system. Section 2 introduces the equations of motion for a simplified model of the system to be experimentally studied. Section 3 describes the physical realization of the system with inerter-based isolation that is considered. Section 4 describes the tests performed on this system and examines the resulting dynamic behavior. Finally, conclusions based on this work are discussed in Section 5.

2 ANALYTICAL MODEL OF INERTER-BASED ISOLATION SYSTEM

A diagram of the two-degree-of-freedom system considered is provided in Figure 1. The inerter in this system is placed between the ground and the base mass, and is assumed to be realized with a lead screw that is connected to a flywheel. The effective mass coefficient, inertance, provided by the inerter is represented by *b*.

The rotational velocity of the inerter's flywheel, ω, can be calculated as the product of the time derivative of the relative displacement of the terminals at the two ends of the device, $\dot{u}_b$, and a coefficient related to the mechanism's physics, α (Hwang et al. 2007, Ikago et al. 2012).

$$\omega = \alpha(\dot{u}_b) \tag{1}$$

$$\alpha = 2\pi/\rho \tag{2}$$

where ρ is the lead-screw lead.

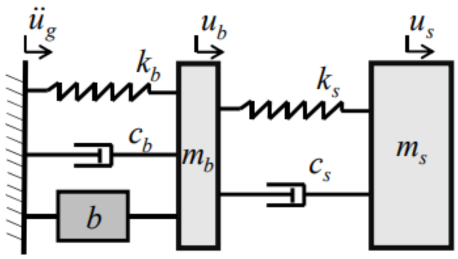

Figure 1. Diagram of system with isolation featuring a rotational inertial damper

The kinetic energy of the inerter will be related to the contribution of the inerter to the system's equations of motion. Because of the small physical mass assumed to be used for the inerter, the kinetic energy related to the translation of the inerter's mass is neglected and the inerter's kinetic energy can be written as:

$$T = \frac{1}{2}J\omega^2 \tag{3}$$

The flywheel used in the experiments in this work has been fabricated as a ring with attached screws; thus, the mass moment of inertia (J) is calculated as:

$$J = (J_1 + J_2 + J_3) \tag{4}$$

where J_1 is the mass moment of inertia from the screws, J_2 is the mass moment of inertia of the ring, and J_3 is the mass moment of inertia of the lead screw. J_1 can be easily changed with different size screws to make the flywheel have a bigger or smaller moment of inertia. By substituting Eq. (1) into Eq. (3), the kinetic energy becomes:

$$T = \frac{1}{2}J\alpha^2(\dot{u}_b)^2 \tag{5}$$

The effective inertial contribution to the system from the inerter will be:

$$\frac{d}{dt}\left(\frac{\partial T}{\partial \dot{u}_i}\right) = J\alpha^2(\ddot{u}_b) \tag{6}$$

All parameters before $\ddot{u}_b$ are considered as the effective mass coefficient, inertance, resulting from the inerter and is referred to as $b = J\alpha^2$. In this study, a smaller and bigger flywheel will be considered with inertance values of 2.32 kg and 28.41 kg, respectively.

Depending on the parameters of the flywheel and lead screw, *b* can be realized by utilizing a small physical mass; thus, the effective mass can be amplified. The resulting equations of motion for the structure are:

$$\begin{aligned} &m_s\ddot{u}_s + c_s(\dot{u}_s - \dot{u}_b) + k_s(u_s - u_b) = -m_s\ddot{u}_g(t) \\ &(m_b + b)\ddot{u}_b + c_s(\dot{u}_b - \dot{u}_s) + c_b\dot{u}_b + k_s(u_b - u_s) + \\ &k_b u_b = -m_b\ddot{u}_g(t) \end{aligned} \tag{7}$$

Where m_s is the primary system mass, m_b is the base mass, b is the effective rotational mass, c_s and k_s are the main structure damping and stiffness, c_b and k_b are the base isolation damping and stiffness, respectively. u_b, u_s, and $\ddot{u}_g$ are the primary system displacement relative to the ground, base displacement relative to the ground and, ground acceleration, respectively.

3 EXPERIMENTAL REALIZATION

The schematic configuration of the experimentally considered system is provided in Figure 2. This figure shows beam springs have been used to realize the stiffness elements in the system. This includes the isolation's low-stiffness connection with the base of the system. Furthermore, a single centralized flywheel connected to the equipment with a lead-screw mechanism provides the isolator's inertance. Guide rods in the setup are used to limit undesired non-vertical motion in the system; however, it should be noted that some horizontal and torsional motion in the system still persist and can be seen in the analysis of its dynamic response. The physical realization of this experimental system is presented in Figure 3.

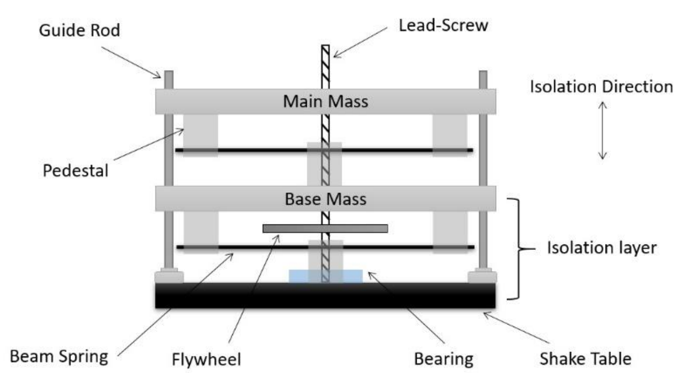

Figure 2. System configuration including isolator configuration with concentrated rotational mechanism paired with beam spring isolators

This system is connected to a shake table. This shake table was used to provide a broadband vertical excitation that was design to be passbanded from 2 to 200 Hz and have a duration of 300 seconds. Tests have been done without the inerter and with two different flywheel sizes (two *b* values). Values of the system parameters are provided in Table 1.

Table 1. System properties

System Parameters	Value	unit
ms	3.13	kg
mb	2.13	kg
ks	870890	N/m
kb	114210	N/m
b (bigger flywheel)	28.41	kg
b (smaller flywheel)	2.32	kg

The structure was instrumented with accelerometers on the shake table and two vertical accelerometers attached to each mass plate.

The results of one accelerometer on the top floor are presented in this study to analyze and show the influence of different isolation configurations on the isolated system's response. The experimental transfer functions presented are calculated considering this accelerometer and the measured ground excitation.

Figure 3. Experimental test setup

4 EXPERIMENTAL RESULTS

The data collected from the tests of the isolated system were processed and evaluated. Some factors can be considered in the analysis to show the effects of using the inerter as a vibration mitigation device. One of the most important is monitoring the transfer function results of different configurations, considering the ground acceleration as the input and the top mass acceleration as the output.

Considering the transfer function results shown in Figure 4, it can be seen that the isolation mode (the first natural frequency) has shifted from 13 Hz with the system with no flywheel, to around 5 Hz using a bigger flywheel and to 10 Hz using the smaller flywheel. In addition to reducing the isolation frequency, it can be seen that the presence of the inerter greatly reduces the peak of the isolation mode with this reduction more with the bigger flywheel.

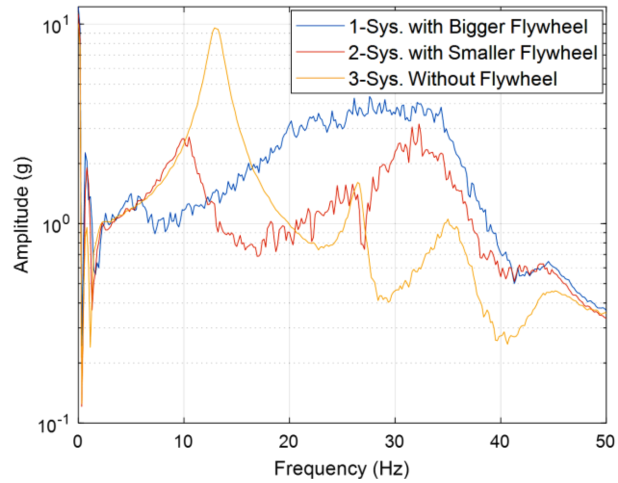

Figure 4. Ground acceleration to top mass acceleration transfer function for different configurations of the inerter

While the inerter greatly reduces the isolation mode, some of the other modes may be made more prominent by the inerter (see Figure 4) and more high frequency noise can result (see Figure 5).

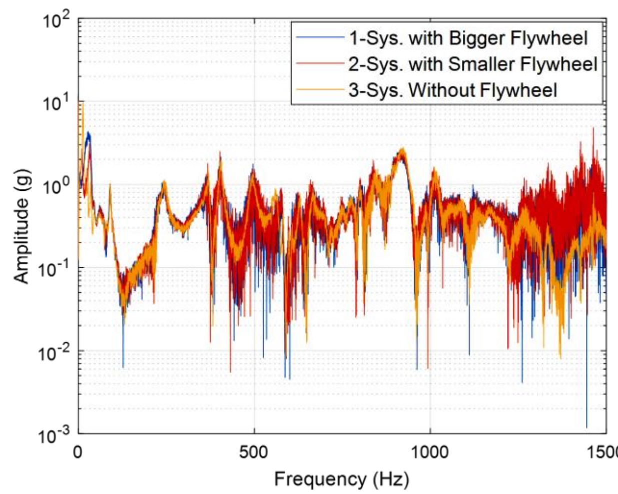

Figure 5. Ground acceleration to top mass acceleration transfer function for different configurations of the inerter shown over a larger frequency range.

The RMS (root mean square) of the acceleration response is examined in Figure 6 and the maximum absolute acceleration is examined in Figure 7. To understand wherein the frequency range where noise in the signal is coming from, lowpass filtering is imposed on the time-history of the results shown in these figures to see how the behavior of the configurations changes during the range by ignoring the higher frequencies. Due to the data acquisition settings, the highest frequency resulted is 5120 Hz. Ten lowpass filter frequencies of 60, 100, 150, 300, 500, 1000, 2000, 3000, 4000, and 4500 Hz were considered.

Examining these figures shows that the noise negatively impacts the performance of the isolation system with the inerter; however, the impact is primarily occurring at higher frequencies. Consequently, if the system considered is not sensitive to higher frequencies, the benefits in isolation mode reduction from the inerter may be worth the tradeoff of some increased noise.

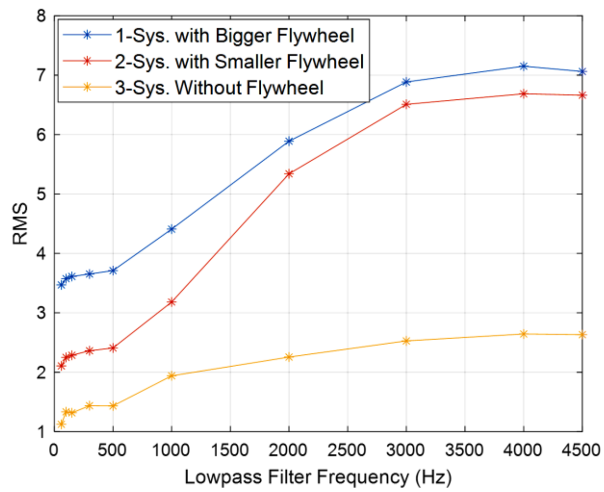

Figure 6. RMS results after considering different passband filter

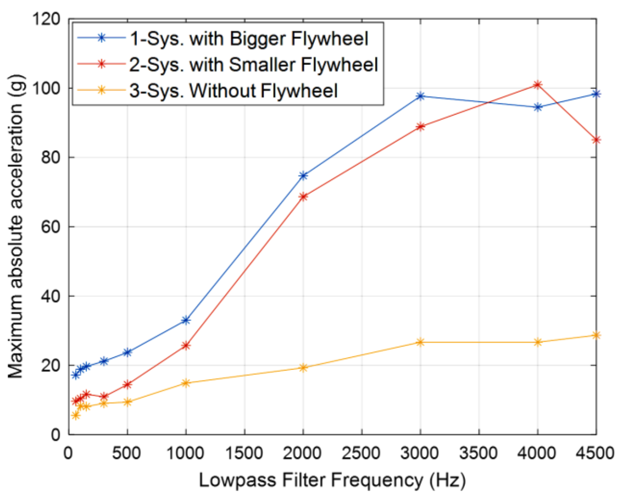

Figure 7. Maximum absolute acceleration considering various filter passband

5 CONCLUSION

The inerter is a device that converts translational motion to rotational motion and in doing so can create large mass effects with only a small amount of physical mass. Inerters have been considered in a variety of structural control methodologies where added mass effects are desired, but the addition of physical mass is not practical. In this paper, the inerter was experimentally considered as part of a base isolation system that is excited by a broadband vertical ground motion. The results of the experimental investigation show that, as expected from analytical models, the effect of the inerter is to reduce the isolation mode frequency. Furthermore, the amplitude of the isolation mode was shown to be significantly reduced. This reduction in isolation mode frequency and amplitude without a reduction in stiffness is ideal for scenarios where a lower isolation frequency is required, but the static deflection or dynamic response of the isolation mode should not be increased. A drawback of using an inerter in the isolation layer was observed when considering the RMS and peak value of the acceleration response due to increased high-frequency response with the inerter. However, as demonstrated by examining the low-pass filtered results, more comparable peak and RMS acceleration results are observed for the systems with and without the inerter given lower cut off frequencies. Consequently, this drawback is significantly less important for systems not sensitive to high frequency response. The results of this work experimentally demonstrate the potential of isolation systems with inerters and encourage their further study.

6 ACKNOWLEDGEMENTS

This material is based upon work supported by NASA under corporative agreement No. 80NSSC20M0185. Any opinions, findings, and conclusions or recommendations expressed in this material are those of the authors and do not necessarily reflect the views of NASA.

7 REFERENCE

Chen, M.Z., Papageorgiou, C., Scheibe, F., Wang, F.C. & Smith, M.C. 2009. The missing mechanical circuit element. *IEEE Circuits and Systems Magazine*, 9(1), pp.10-26.

Chen, M.Z., Hu, Y., Huang, L. & Chen, G. 2014. Influence of inerter on natural frequencies of vibration systems. *Journal of Sound and Vibration*, 333(7), pp.1874-1887.

Hwang, J.S., Kim, J. & Kim, Y.M. 2007. Rotational inertia dampers with toggle bracing for vibration control of a building structure. *Engineering Structures*, 29(6), pp.1201-1208.

Ikago, K., Saito, K. & Inoue, N. 2012. Seismic control of SDOF structure using tuned viscous mass damper. *Earthquake Engineering and Structural Dynamics*; 41:453–474.

Javidialesaadi, A. & Wierschem N.E. 2018. Optimal design of rotational inertial double tuned mass dampers under random excitation. *Engineering Structures*; 165: 412–421. DOI: 10.1016/j.engstruct.2018.03.033.

Marian, L. & Giaralis, A. 2014. Optimal design of a novel tuned mass-damper–inerter (TMDI) passive vibration control configuration for stochastically support-excited structural systems. *Probabilistic Engineering Mechanics*; 38: 156–164. DOI: 10.1016/j.probengmech.2014.03.007.

Smith, M.C. 2002. Synthesis of mechanical networks: the inerter. *IEEE Transactions on Automatic Control*; 47:1648–1662.

Wang, F.C., Chen, C.W., Liao, M.K. & Hong, M.F. 2007. Performance analyses of building suspension control with inerters, *Proceedings of the 46th IEEE Conference on Decision and Control*: New Orleans, LA, USA; 3786–3791.

Wang, F.C., Hong, M.F., Chen, C.W. 2009. Building suspensions with inerters. Proceedings IMechE, *Journal of Mechanical Engineering Science*; 224:1605–1616.